Journal of Polymer Research (2023) 30:403
https://doi.org/10.1007/s10965-023-03780-w

ORIGINAL PAPER

Self-driven directional polypyrrole-polyethyleneimine nanopigment-infused medical textiles with potential asymmetrical ionic convection and biological effects for follicle restoration

Sih-Chi Chuang[1] · Shih-An Yu[2] · Pei-Chia Hung[2] · Chih-Wei Chiang[3] · Wen-Ta Su[1] · Pei-Ru Jheng[4] · Wei-Yung Huang[4] · Ping-Chien Hao[4] · Jia Wei Liang[4] · Yung-Wei Lin[5,6,7] · Hsu-Wei Fang[1] · Er-Yuan Chuang[4,8,9]

Received: 10 June 2023 / Accepted: 14 September 2023 / Published online: 13 October 2023
© The Polymer Society, Taipei 2023

Abstract

Hair loss is one of the most common and distressing conditions that can be traumatic for an individual. Many non-pharmacological and pharmacological treatments for hair loss have been developed. However, serious side effects or limitations in terms of the hair regeneration potential still exist. One of the non-pharmacological treatments, biophysical stimulation, has shown promise in hair regeneration. Nevertheless, the associated discomfort and the need for external components such as an electrical power supply pose challenges to its widespread use. In this study, we present an innovative cationic fabric that utilizes repeatable asymmetrical ionic flow of a physiological fluid to internally stimulate hair follicles and skin. Characterization, ultrasonic, biochemical, and histological experiments were conducted. The use of this developed treatment significantly increased expressions of heat shock proteins and potentially improved immunoregulation in the skin, as well as increased the number of hair follicles in skin defect animals, with no adverse risks.

Keywords Polypyrrole-polyethyleneimine nanopigment-woven medical product · Asymmetrical ionic convection · Heat-shock protein · Immunomodulation · Follicle repair

Sih-Chi Chuang, Shih-An Yu, Pei-Chia Hung, Chih-Wei Chiang, Pei-Ru Jheng, and Wei-Yung Huang contributed equally to this work.

✉ Yung-Wei Lin
yungweilin@tmu.edu.tw

✉ Hsu-Wei Fang
hwfang@ntut.edu.tw

✉ Er-Yuan Chuang
eychuang@tmu.edu.tw

[1] Department of Chemical Engineering and Biotechnology, National Taipei University of Technology, Taipei 10608, Taiwan

[2] Hsuan Chen Technology Co., Ltd., New Taipei City 22055, Taiwan

[3] Bone and Joint Research Center, Department of Orthopedics, Taipei Medical University Hospital, School of Medicine, College of Medicine, Taipei Medical University, Taipei 11031, Taiwan

[4] Graduate Institute of Biomedical Materials and Tissue Engineering, Taipei Medical University, Taipei 11031, Taiwan

[5] International Master/Ph.D. Program in Medicine, College of Medicine, Taipei Medical University, Taipei 11031, Taiwan

[6] Department of Urology, School of Medicine, College of Medicine and TMU Research Center of Urology and Kidney (TMU-RCUK), Taipei Medical University, Taipei 11031, Taiwan

[7] Department of Urology, Wan Fang Hospital, Taipei Medical University, Taipei 11696, Taiwan

[8] Cell Physiology and Molecular Image Research Center, Taipei Medical University-Wan Fang Hospital, Taipei 11696, Taiwan

[9] International Ph.D. Program in Biomedical Engineering, College of Biomedical Engineering, Taipei Medical University, Taipei 11031, Taiwan

Introduction

Hair loss is a common and distressing condition worldwide. Although the exact cause of hair loss is not fully understood, it is known that various factors, including stress and heredity, can negatively affect hair shafts and follicles, which are complex mini-tissues of the skin [1]. Current medical treatments for hair loss, such as finasteride and minoxidil [2, 3], approved by the US Food and Drug Administration (FDA), can help slow down hair loss but do not significantly increase the number of hair follicles. However, these medications can have unwanted side effects on the body [4, 5]. As alternatives, non-pharmacological biophysical stimulation methods are being explored, as they are considered biocompatible and low-risk therapies for hair regeneration and regrowth. These methods mainly include electric stimulation and low-level laser therapy [6–9].

In maintaining hair cycle homeostasis, hair follicles go through stages of anagen (hair growth), catagen (destruction), and telogen (rest), and "maintenance" of this hair cycle is crucial for preventing hair loss [10]. Therefore, biophysical stimulation can be a valuable tool for maintaining, and regulating the bioactivity of cells, proteins, and substances related to hair regeneration without adverse risks [11].

Specifically, electric stimulation affects various processes from cellular proliferation to differentiation by enhancing ion transport and adenosine triphosphate (ATP) production [12, 13], potentially improving the local circulation, activating key proteins, polarizing immune cells, promoting keratinocyte proliferation, enhancing the bioactivity of hair follicle dermal papilla cells, and preventing depletion of stem cell progeny and pools [14, 15]. Electric stimulation-based therapies show great promise as future biomedical techniques. However, current methods of electric stimulation have limitations, such as poor clinical effectiveness and the need for an external electrical power supply, which hinder their application to hair follicles.

In real-world scenarios, the requirement for an external power source creates user limitations and inconvenience in daily use. Therefore, a novel therapeutic approach is needed that can be used daily, has minimal risks, is battery-free, and is suitable for hair loss therapy. Although several portable electric stimulation devices without external power sources were reported [16, 17], there is still a lack of research on electric stimulation strategies for hair loss. Additionally, scalp stimulation provided by current wearable or portable devices poses challenges, as the effectiveness of stimulation can be significantly reduced due to the need for specific head movements or the inability to stimulate cells involved in the hair cycle that are located deep within the hair bulb.

It is well-known that the human body has a cellular biological electrical system that generates intrinsic electrochemical signals in various parts, such as the skin, brain, heart, muscles, and bones. In physiological aqueous solutions, an electrical current is carried by charged ions, as there are no free electrons available [18]. Within the skin, asymmetric ionic flows, similar to "electrophoresis," produce naturally occurring electrical potentials that dissipate without being harnessed. Therefore, a self-driven directional potential, known as a "skin battery," generated by repeatable asymmetric ion movement around areas affected by hair loss, was proposed as a hair follicle stimulation system without the need for external electrical power sources or additional electrical components.

Here, a strategy involving repeatable asymmetric ion flow was established using cationic polypyrrole (PPy)-polyethylenimine (PEI) nanopigments (NPs) coated onto a polyethylene (PE) fabric commonly used in medicine. This coated fabric is referred to as PE fabric-PPy-PEI NPs. In this study, we elaborate the workability of the mechanism of repeatable asymmetric ion flow and potential transfer from intermediate physiological fluids to the skin, mediated by PE fabric-PPy-PEI NPs (Fig. 1). Additionally, the study examined the asymmetric ion behavior induced by PE fabric-PPy-PEI NPs, which potentially involved ion and deposition of potential electrodes or substances. Furthermore, the study assessed the biological induction of heat-shock protein (HSP) expressions by cationic PE fabric-PPy-PEI NPs, which could be as therapeutic agent [19] or help moderate immune responses and inhibit inflammation. In an in vivo skin defect model, this study investigated the potential effects of PE fabric-PPy-PEI NPs of regulating HSPs, macrophages, anti-inflammation, and hair growth.

Experimental section

Fabrication of the PE fabric-PPy-PEI NPs

The PE fabric-PPy-PEI NPs were fabricated following a previously reported method [20]. In brief, 200 mg of PEI (0.6 kDa, catalog no. 408,719; Sigma-Aldrich) was diluted in 20 mL of deionized (DI) H_2O, and the aqueous solution was adjusted to an acidic environment (pH 0.8), using 6 M hydrochloric acid. Next, the solution was mixed with a pyrrole monomer (12.5 µl, catalog no. 131,709; Sigma-Aldrich), and 1 mL of ferric chloride hexahydrate (12.5 mg/mL) was added dropwise. After 0.5 h of polymerization, the resulting black solution was dialyzed several times using a 3500-Da molecular weight cutoff (MWCO) dialysis membrane against DI H_2O for 3 days to remove free PEI and excess ferric ions and obtain PPy-PEI NPs. To prepare the PE fabric-PPy-PEI NPs, a piece of medical-grade PE fabric was soaked in a 10 mg/mL PPy-PEI NPs solution for

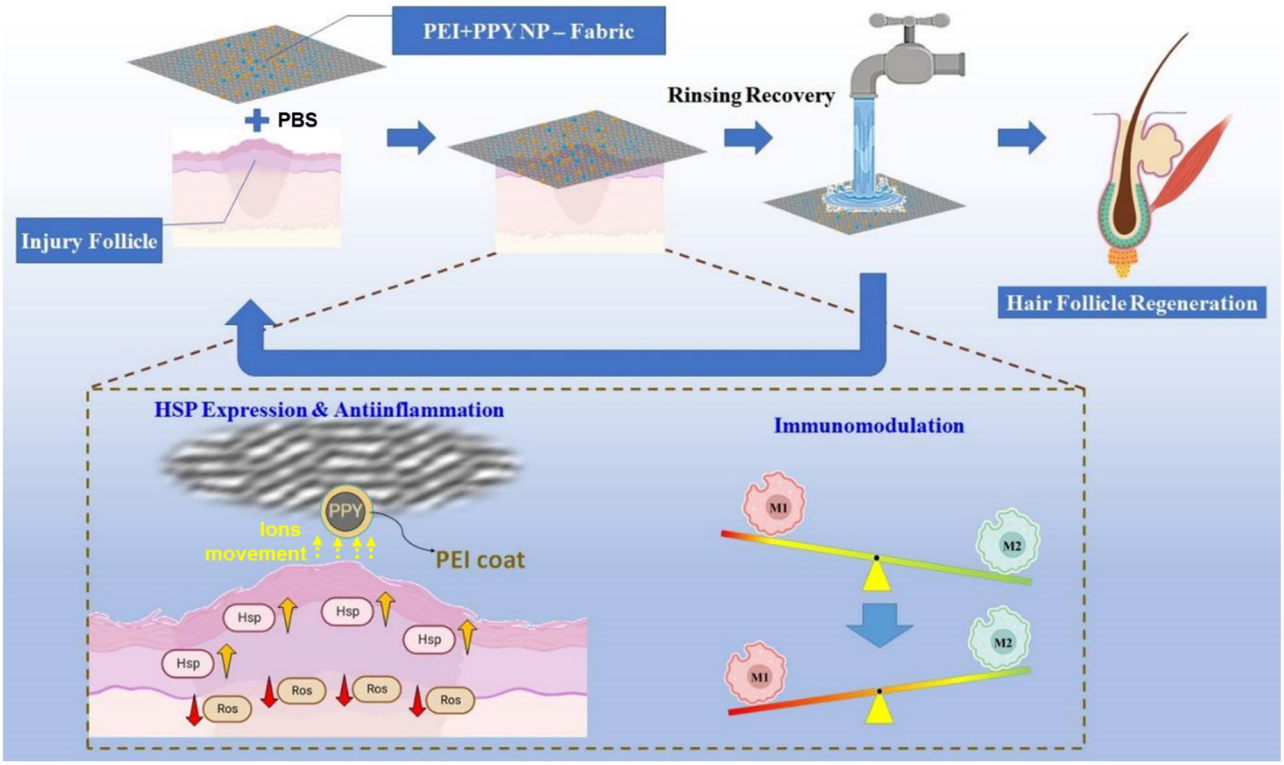

Fig. 1 Schematic illustration depicting that the polyethylene (PE) fabric-polypyrrole (PPy)-polyethylenimine (PEI) nanopigments (NPs) are expected to create repeatable asymmetric ion flow, heat shock protein (HSP) amplification, immunomodulation, and anti-inflammation in a drug- and power-free manner to biophysically stimulate follicle repair. The illustration was partially made using Biorender.com

48 h, following a previously published polymeric coating method [20]. To prepare PE fabric-PEI, the same PE fabric was soaked in a 10 mg/mL PEI solution for 48 h. The resulting PE fabric-PEI or PE fabric-PPy-PEI NPs were washed three times with DI H_2O for further use.

Characterization

Particle size and size distribution of PPy-PEI NPs were determined using dynamic light scattering (DLS, Malvern). The zeta potential values of PPy-PEI NPs were measured using DLS data.

Mechanical properties of the PE fabric, PE fabric-PEI, and PE fabric-PPy-PEI NP samples were assessed. The test was performed using a Dynamic Mechanical Analyzer (DMA, Q800 T.A. Instruments).

For the scanning electron microscopic (SEM) analysis, test samples (PE fabric, PE fabric-PEI, or PE fabric-PPy-PEI NPs) were sliced into pieces approximately 0.5 mm thick and 3 mm wide. Afterward, samples were observed using a Hitachi SU3500 field emission scanning electron microscope (SEM) operating at 15 kV. Imaging was conducted using both back-scattered and secondary electron signals.

An energy dispersive spectroscopic (EDS) analysis was performed to detect and quantify elements present in the samples (PE fabric, PE fabric-PEI, or PE fabric-PPy-PEI NPs). The process was the same as that described for SEM testing. Briefly, sliced samples were observed using a Hitachi SU3500 microscope at 15 kV. Mapped images were used to record the presence of chemical ingredients in each sample. The extent of each element was quantitatively detected, calculated, and measured at four random points. Vapor permeability and the water content of the test fabrics were referred to using a previously established method [20].

To measure the flow/movement of charged substances in physiological fluid and assess whether PE fabric-PPy-PEI NPs could drive repeatable asymmetric ion flow through reversible absorption and desorption behaviors, a detection assay using fluorescein isothiocyanate (FITC), a charge-bearing fluorescent indicator, was employed. In this study, 0.1 mg/mL of FITC was dispersed in pH 7.4 phosphate-buffered saline (PBS), and test samples (PE fabric, PE fabric-PEI, or PE fabric-PPy-PEI NPs) were immersed in the FITC PBS solution. The absorption and desorption behaviors of fluorescent FITC from the test samples were detected using a fluorescence microscope (Leica DMi8).

In vivo studies

The in vivo experiments were approved by the Animal Care and Use Committee of Taipei Medical University. Male ICR mice (with body weights of about 23 g) were purchased from BioLASCO (Taipei, Taiwan) and was housed for 7 days prior to the animal experiment. The hair of ICR mice on the dorsal skin was removed with an animal razor, and the animals were anesthetized with 1%~4% isoflurane by inhalant administration, and their shaved skin was sterilized with 70% alcohol. To create a thermal-induced follicular injury method [21], a 90 °C metal rod was placed on the shaved skin for 15 s.

After thermal-induced follicular injury, PE fabric-PPy-PEI NPs were placed on the back of the skin-damaged ICR mice, which was rinsed with 1 mL PBS, during the experiment. A group of mice with PBS treatment was included as a control. To maintain the maximal current potential for asymmetric ionic flows on the lesioned skin, PBS was replaced three times a day, while substituted PE fabric-PPy-PEI NPs were frequently (every 4 h) soaked in/washed by DI water to release saturated charged ions from the membrane through a mass or ionic gradient for 1 h at room temperature.

Four days later, animals were anesthetized and sacrificed with CO_2. Dorsal skin (1 × 2 cm) was rapidly collected and fixed with 10% formaldehyde. Tissues (skin, heart, liver, kidneys, lungs, and spleen) were cut into about 5-μm slices and stained with hematoxylin and eosin (H&E) to evaluate the epidermis thickness. A histological microscopic analysis was performed using an optical microscope (Leica, DMi8). Morphological changes in the epidermis of skin tissues were determined.

To investigate the biochemical properties of the test skin samples, protein markers of HSP, M1 macrophages, and M2 macrophages in skin tissues were determined using an immunofluorescence method, following the manufacturer's protocol. Primary antibodies used were a fluorescently-conjugated anti-HSP70 antibody (37 °C, 1 h, 1:100), anti-CD86 (M1) antibody (37 °C, 1 h, 1:100), and anti-CD206 (M2) antibody (37 °C, 1 h, 1:100). Then, slices were washed with PBS three times for 5 min. Nuclei were stained with 4',6-diamidino-2-phenylindole (DAPI) (37 °C, 20 min, 1:500). A 2',7'-dichlorodihydrofluorescein diacetate (DCFH-DA) fluorescent assay was used to monitor cellular reactive oxygen species (ROS) levels in skin tissues [22, 23]. Fluorescently stained slides were observed with a fluorescent microscope (Leica, DMi8).

Statistical analysis

Quantitative data are presented as the mean ± error bar. GraphPad Prism 6 software was utilized to check statistical differences. A p value of <0.05 was defined as statistically significant.

Results and discussion

PE fabric-PPy-PEI NP preparation and characterization

Distribution profiles of Fig. 2a reveal that PPy-PEI NPs had a positive charge (+52.8 mV) and an average hydrodynamic diameter of ca. 355 nm. The mechanical properties of PE fabric, PE fabric-PEI, and PE fabric-PPy-PEI NPs were studied by DMA, and results are shown in curves of Fig. 2b. PE fabric-PPy-PEI NPs possessed higher mechanical properties compared to PE fabric or PE fabric-PEI.

Microscopic data (Fig. 2c) showed that PE fabric, PE fabric-PEI, and PE fabric-PPy-PEI NPs had a mesh microstructure which would allow a vapor permeability ability. SEM-EDS data suggested that the PPy-PEI NPs seemed to be distributed on the fiber surface of the PE fabric, and organic elements of the PE fabric, PE fabric-PEI, and PE fabric-PPy-PEI NPs are shown in Fig. 2d. Results of the water content (Fig. 2e) and vapor permeability (Fig. 2f) confirmed that PE fabric, PE fabric-PEI, and PE fabric-PPy-PEI NPs had water-absorption abilities (above 30%) and vapor permeability (of ca. 0.2 mg/min). Both the water-absorption ability and vapor permeability are important factors for fabric comfort [24, 25].

Ionic absorption and desorption behaviors in physiological fluid are two significant index parameters for applications of asymmetrical ionic convection or flow. Analyzing ionic absorption and desorption behaviors using charged fluorescent FITC kinetic models is an efficient way to investigate kinetic mechanisms. Fluorescent microscopic data (Fig. 3) showed that after PE fabric-PEI was soaked in an FITC-containing PBS solution, the higher green fluorescent FITC signal was absorbed onto the surface of fabric-PEI, which was higher than that of the PE fabric group. It is possible that the cationic PEI can capture anionic FITC [26], through potential electrostatic interactions. The PE fabric-PPy-PEI NP group showed the greatest FITC absorption ability, compared to the PE fabric and PE fabric-PEI groups. This was likely due to the existence of PPy as an additional ionic reservoir to store much more anionic/charged substances (e.g., FITC or chloride ions), thus creating a maximal current potential plus asymmetrical ionic convention or flow in the lesion microenvironment with PBS. After FITC had been absorbed onto the PE fabric-PPy-PEI NPs, they were immersed and washed with water, and owing to the ionic gradient, the FITC was desorbed from the PE fabric-PPy-PEI NPs, according to Fig. 3. Thus, this PE Fabric-PPy-PEI NPs had ionic absorption and desorption properties in a repeatable manner, potentially driving a maximal current potential plus asymmetrical ionic convention or flow for local stimulation and follicle repair, which was found to be feasible.

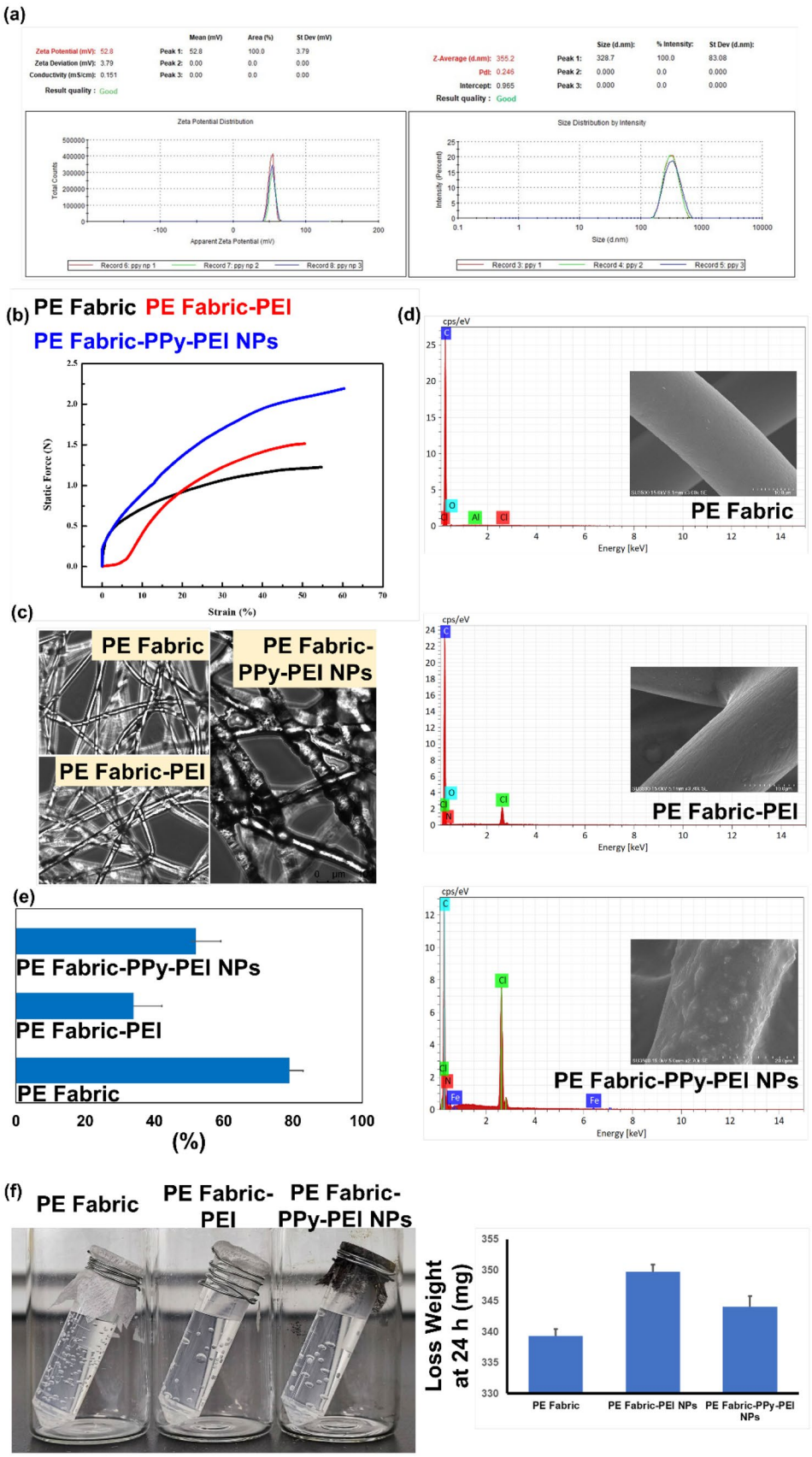

Fig. 2 Characterization. **a** DLS data for the zeta potential and particle size of polypyrrole (PPy)-polyethyleneimine (PEI) nanopigments (NPs). **b** DMA, **c** microscopic, **d** scanning electron microscopy-energy-dispersive x-ray spectroscopy (SEM-EDS), **e** water content analysis, and **f** vapor permeability analyses of polyethylene (PE) fabric, PE fabric-PEI, and PE fabric-PPy-PEI NPs. ($n \geq 3$)

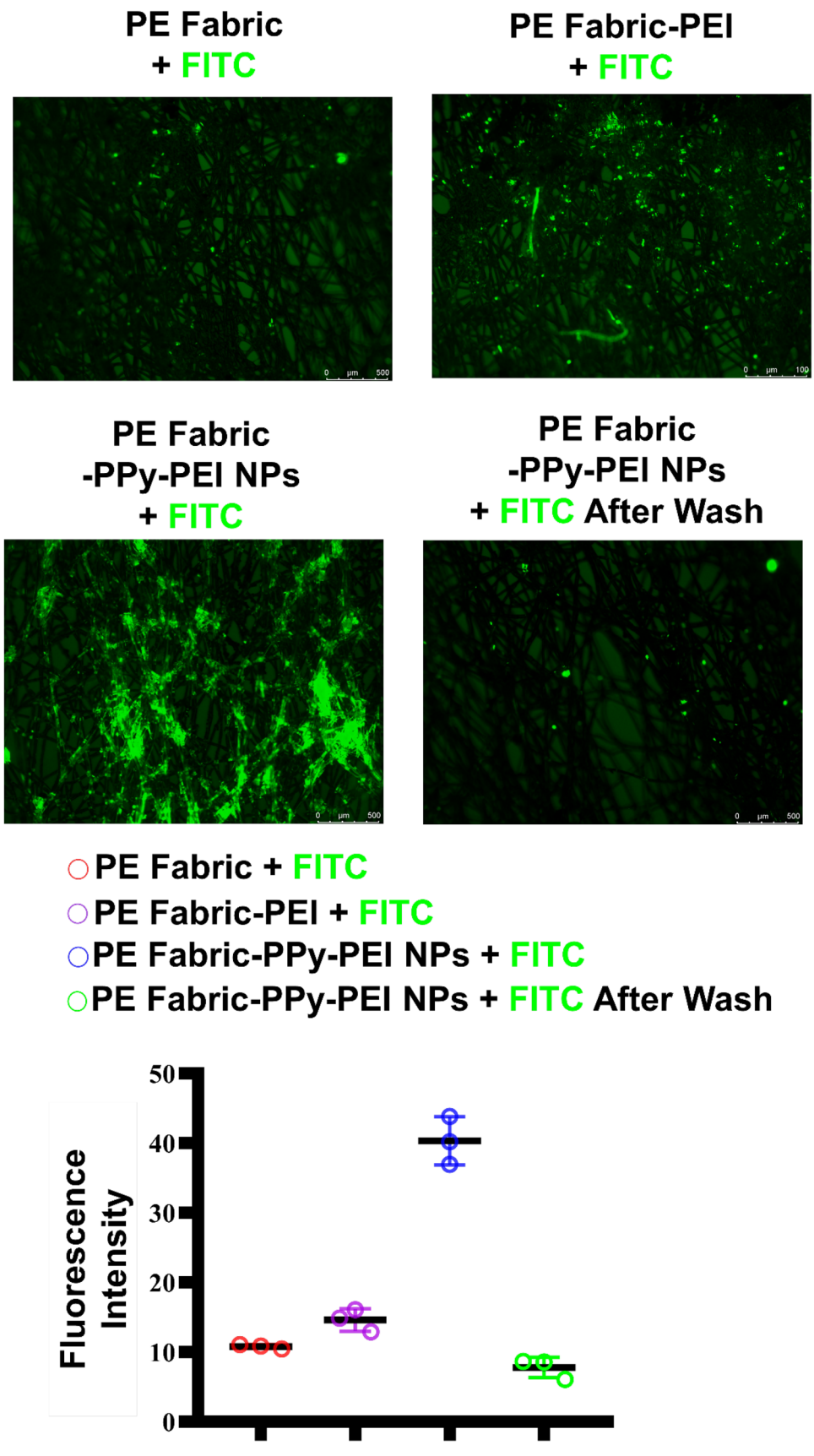

Fig. 3 Ionic absorption and desorption behaviors of PE fabric-polypyrrole (PPy)-PEI nanopigments (NPs) using a fluorescent fluorescein isothiocyanate (FITC) assay

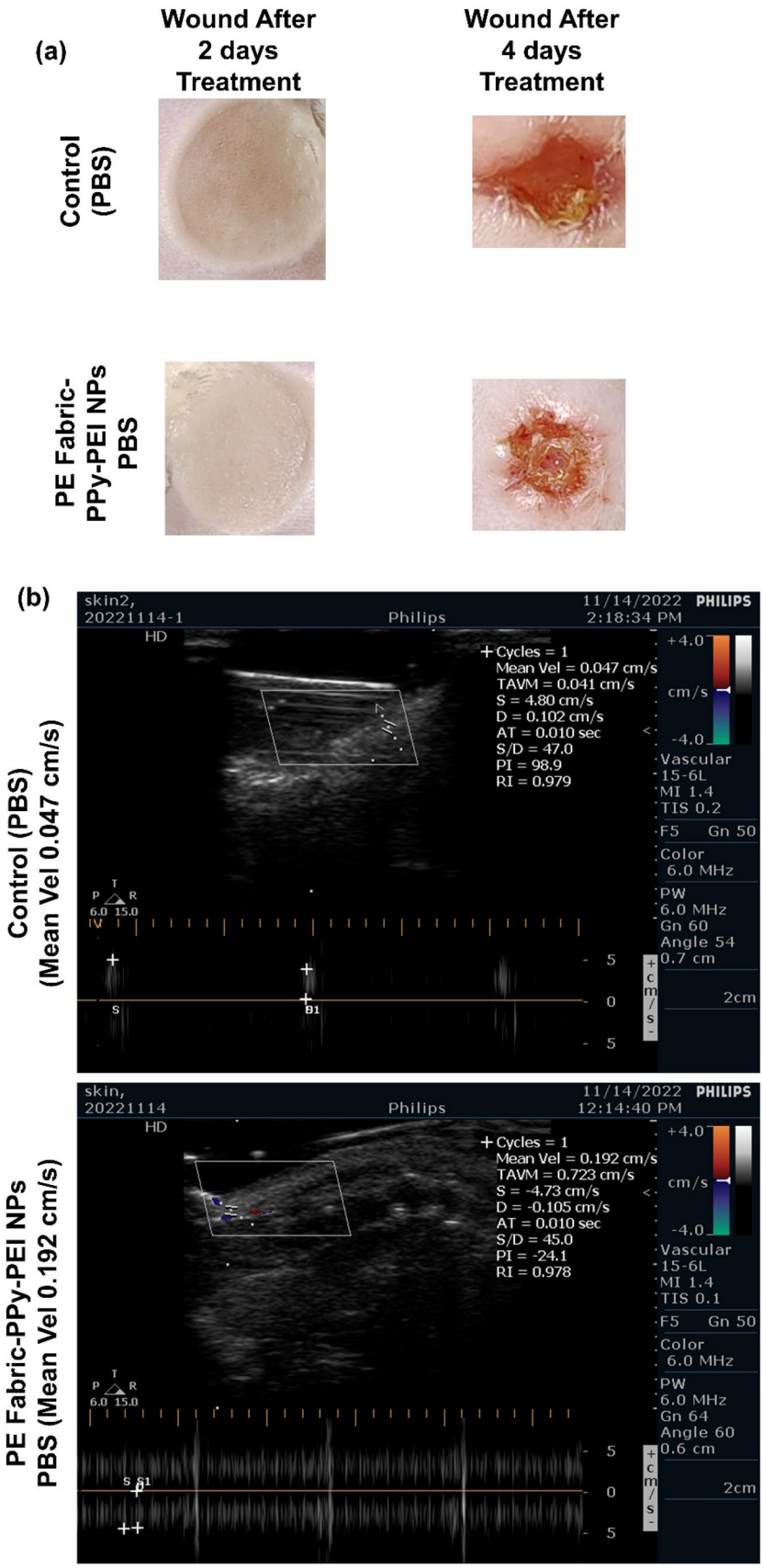

Fig. 4 In vivo studies. **a** Animal study of different formulations (PBS or PBS plus polyethylene (PE) fabric-polypyrrole (PPy)-polyethyleneimine (PEI) nano-pigments (NPs)) and wound observation. **b** Ultrasound experimental data

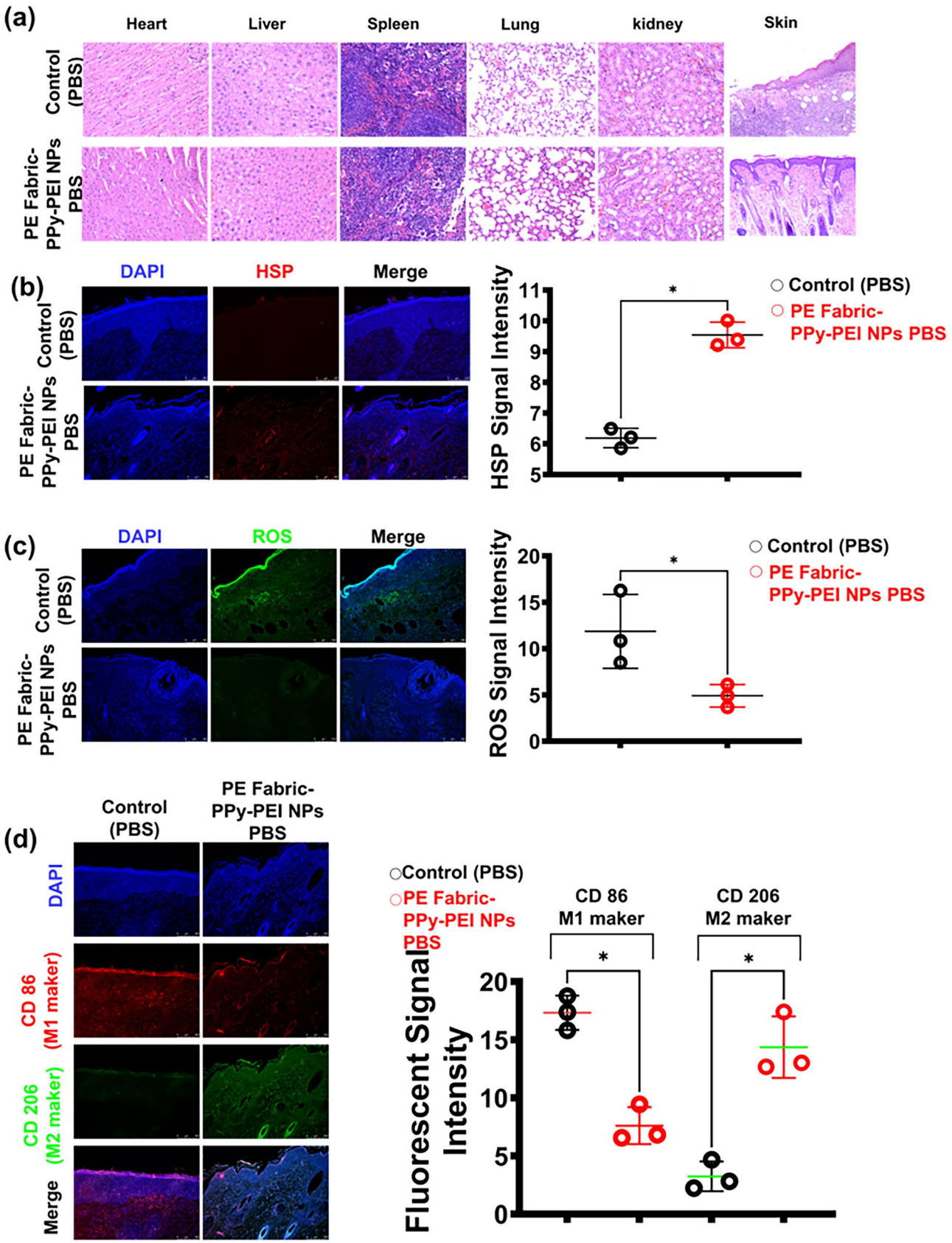
(a)
Heart
Liver
Spleen
Lung
kidney
Skin
Control (PBS)
PE Fabric-PPy-PEI NPs PBS
(b)
DAPI
HSP
Merge
Control (PBS)
PE Fabric-PPy-PEI NPs PBS
HSP Signal Intensity
11
10
9
8
7
6
5
*
Control (PBS)
PE Fabric-PPy-PEI NPs PBS
(c)
DAPI
ROS
Merge
Control (PBS)
PE Fabric-PPy-PEI NPs PBS
ROS Signal Intensity
20
15
10
5
0
*
Control (PBS)
PE Fabric-PPy-PEI NPs PBS
(d)
Control (PBS)
PE Fabric-PPy-PEI NPs PBS
DAPI
CD 86 (M1 maker)
CD 206 (M2 maker)
Merge
Control (PBS)
PE Fabric-PPy-PEI NPs PBS
CD 86 M1 maker
CD 206 M2 maker
Fluorescent Signal Intensity
20
15
10
5
0
*
*

◂**Fig. 5** Histological studies. **a** H&E staining of tissues (heart, liver, spleen, lungs, kidneys, and skin). Skin immunofluorescence staining for **b** heat shock protein (HSP), **c** DCFH-DA assay for reactive oxygen species (ROS), and **d** M1/M2 macrophages of test groups (PBS or PBS plus polyethylene (PE) fabric-polypyrrole (PPy)-polyethyleneimine (PEI) nanopigments (NPs)) ($n = 3$)

In vivo studies

We created a thermal-induced full-thickness-follicle, wounded-skin ICR mouse model to evaluate the in vivo skin-wound-repair efficacy, follicle-repair mechanism, and healing effect of the biomaterials (Fig. 4). Encouraged by the in vitro results, the PE fabric-PPy-PEI NPs were chosen for the efficiency of follicle repair and wound treatment. Obviously, the skin wound area was progressively attenuated with prolongation in both groups (Fig. 4a). In particular, the PE fabric-PPy-PEI NPs plus PBS group seemed to have regular wound closure compared to the PBS control group (Fig. 4a). Compared to a previously reported PPy-loaded system, our prepared PPy-PEI NP-based matrix possessed wound-healing potential [22, 23, 27].

Doppler ultrasound (Fig. 4b) is a remote, noninvasive analysis that can be used to estimate blood flow and circulation through blood vessels by bouncing high-frequency sound waves from ultrasound off circulating red blood cells. As shown in the in vivo ultrasonic data (Fig. 4b), skin lesion in the fabric-PPy-PEI NPs plus PBS group showed increased blood flow (0.192 cm/s), compared to that of the PBS control group (0.047 cm/s). The local increase in blood flow might supply more nutrients and oxygen to peripheral areas.

Stimulation is exploited in clinical practice to relieve acute and chronic pain. It is thought that stimulation of peripheral tissues increases blood flow and can aid healing. The cationic fabric-PPy-PEI NPs might facilitate the asymmetrical ionic flow in PBS, as indicated in Fig. 1. When the cationic fabric-PPy-PEI NPs plus PBS were applied to an anionic follicle-damaged skin lesion, this might generate an ionic current potential. The generated ionic current potential possibly speeded up the local mass transportation rate, thus leading to a rise in the available exchange area for nutrients, oxygen, growth factors, hormones, and waste products (e.g., lactic acid, hydrogen ions, and so on). A previously developed transcutaneous electrical tissue stimulation technique was found to locally increase blood flow and vascular endothelial growth factor levels in both healthy and diabetic conditions [28–30].

A series of pathological examinations was carried out to further investigate follicle- and wound-healing processes (Fig. 5). Moreover, no apparent injury was observed in the major organ tissues (heart, liver, spleen, lungs, or kidneys) stained with H&E (Fig. 5a). Overall, these data indicated that the outcome mediated by fabric-PPy-PEI NPs + PBS could have in vivo biosafety. In the PBS control group, skin wounds exhibited a lower regenerating epidermis, which appeared more irregular compared to wounds treated with fabric-PPy-PEI NPs + PBS. Additionally, follicular morphology seemed to be rarely observed in the PBS control group.

HSPs are known to function biologically as molecular chaperones, and they not only regulate numerous processes of protein biogenesis but also bio-functions as lifeguards against proteotoxic stresses. By modulating wound clearance of debris, inflammation, cell proliferation and migration, and synthesis of collagen, HSP, as biophysical therapy, is essential for healing skin wounds [31]. Cationic biomaterials/substances can be used to induce the expression of cellular HSP [32], and an increase in HSP was indicated in the presence of cations. Fluorescent microscopic data showed that skin lesions which received fabric-PPy-PEI NPs + PBS exhibited increased skin HSP levels, compared to the PBS control group (Fig. 5b). HSP might get involved with moderating immune responses and inflammation, according to previously published findings [33, 34]. Several findings in animal models and human clinical trials revealed the immunoregulatory efficacies of HSP and its protective function in inflammatory diseases [33].

Additionally, as the late phase of wound healing progressed, hypoxia was reduced and the ROS level decreased [35]. Whereas, elevated and sustained ROS were found in vivo and were associated with chronically impaired wound repair and non-healing wounds [36]. The accumulation of ROS, therefore, is one of the essential bioindicators for characterizing the follicle- and wound-healing process. We thus further examined the ROS level of skin tissues via a DCFH-DA assay. In the experiment, ROS were marked green, and the relative intensity indicated the ROS content. ROS (green) were most extensively distributed in wound beds in the PBS control group (Fig. 5c). In contrast, the distribution was less extensive in the fabric-PPy-PEI NP + PBS group, which suggested that the development of oxidative stress-caused inflammation was inhibited in the fabric-PPy-PEI NP plus PBS group.

In this study, CD86 (a marker of M1 macrophages) and CD206 (a marker of M2 macrophages) were used as markers to identify the immunomodulatory ability of fabric-PPy-PEI NPs. Double immunofluorescence staining of CD86 and CD206 confirmed that expressions of macrophages in the PBS control and fabric-PPy-PEI NP + PBS groups differed (Fig. 5d). Expression of CD86 in the PBS control group was the higher than that in the fabric-PPy-PEI NP + PBS group. In contrast to the PBS control group, large areas of CD206 expression appeared in the fabric-PPy-PEI NP + PBS group. The fabric-PPy-PEI NP + PBS group could potentially polarize M1 macrophages to M2 macrophages, regulate HSP, and reduce ROS.

The current study suggested that M2 macrophages play a vital role in hair growth and wound healing [37].

Conclusions

In summary, we developed and characterized PE fabric-PPy-PEI NPs for follicle regeneration. The combination of PE fabric-PPy-PEI NPs and PBS could promote follicle repair and the wound-healing process through potential asymmetrical ionic flow and biological effects. Our studies demonstrated that fabric-PPy-PEI NPs exhibited biological potential to be utilized in biomedical applications such as hair growth and skin tissue engineering. This study should provide a novel and practical approach, highlighting the follicle- and wound-repair effects of the prepared fabric-PPy-PEI NP system, making this system a promising candidate for biomedical translation in the field of skin tissue engineering. Despite the promising potential of the current technique involving PE fabric-PPy-PEI NPs plus PBS for hair growth, it is crucial to thoroughly investigate the underlying biological mechanisms. In the future, careful attention must be given to quality control and scaling up the production of PE fabric-PPy-PEI NPs.

Acknowledgements This scientific research was financially supported by grants from the National Science and Technology Council (NSTC), Taiwan (111-2320-B-038-039, 112-2221-E-038-002-MY3, and 112-2622-E-038-006-) and University System of Taipei Joint Research Program and Taipei Medical University (USTP-NTUT-TMU-105-08).

Data availability The data supporting the findings of this study are available upon reasonable request from the corresponding author.

Declarations

Conflicts of interest All authors declare that no conflicts of interest exist.

References

1. Schneider MR, Schmidt-Ullrich R, Paus R (2009) The hair follicle as a dynamic Miniorgan. Curr Biol 19:R132–R142
2. Kaufman KD, Olsen EA, Whiting D, Savin R, DeVillez R, Bergfeld W, Price VH, Van Neste D, Roberts JL, Hordinsky M, Shapiro J, Binkowitz B, Gormley GJ, Asarch R, Birchall N, Boersma IH, Brenner S, Bruno K, Buntin D, Burg G, Cilliers J, Cotterill P, Cunliffe WJ, Ferguson D, Fiedler V, Fivenson D, Funicella T, Gencheff C, Gratton D, He W, Horwitz S, Imperato-McGinley J, Santa-Cruz FJ, Katz I, Kelly AP, Kopera D, Kotey P, Lachapelle JM, Ling M, Lopez-Bran E, Lowe N, Lucky A, Hull SM, McDonagh A, Mork C, Peck G, Prens E, Reygagne P, Rietschel R, Rittmaster R, Round E, Rufli T, Sadick N, Saiag P, Sanchez-Pedreno P, Schmidt JB, Sher M, Shupack J, Steiner D, Stewart D, Stiller M, Stough D, Swinehart J, Swinyer L, Todd G, Unger W, Waldstreicher J, Weinstein G, Weiss D, Weiss J, Whitmore SE, Wolff H (1998) Finasteride in the treatment of men with androgenetic alopecia. J Am Acad Dermatol 39:578–589
3. Suchonwanit P, Thammarucha S, Leerunyakul K (2019) Minoxidil and its use in hair disorders: a review. Drug Des Devel Ther 13:2777–2786
4. Rossi A, Cantisani C, Melis L, Iorio A, Scali E, Calvieri S (2012) Minoxidil use in dermatology, side effects and recent patents. Recent Pat Inflamm Allergy Drug Discovery 6:130–136
5. Thompson IM, Goodman PJ, Tangen CM, Lucia MS, Miller GJ, Ford LG, Lieber MM, Cespedes RD, Atkins JN, Lippman SM, Carlin SM, Ryan A, Szczepanek CM, Crowley JJ, Coltman CA Jr (2003) The influence of finasteride on the development of prostate cancer. N Engl J Med 349:215–224
6. Chen Y, Liu L, Fan J, Zhang T, Zeng Y, Su Z (2022) Low-level laser treatment promotes skin wound healing by activating hair follicle stem cells in female mice. Lasers Med Sci 37:1699–1707
7. Pinto GM, Damasco P (2021) Lasers and new technologies in hair diseases. Techniques in the evaluation and management of hair diseases 80–92
8. Yao G, Jiang D, Li J, Kang L, Chen S, Long Y, Wang Y, Huang P, Lin Y, Cai W, Wang X (2019) Self-activated electrical stimulation for effective hair regeneration via a Wearable Omnidirectional Pulse Generator. ACS Nano 13:12345–12356
9. Yan L, Kageyama T, Zhang B, Yamashita S, Molino PJ, Wallace GG, Fukuda J (2022) Electrical stimulation to human dermal papilla cells for hair regenerative medicine. J Biosci Bioeng 133:281–290
10. Ji S, Zhu Z, Sun X, Fu X (2021) Functional hair follicle regeneration: an updated review. Signal Transduct Target Therapy 6:66
11. Hu M, Hong L, He S, Huang G, Cheng Y, Chen Q (2020) Effects of electrical stimulation on cell activity, cell cycle, cell apoptosis and β-catenin pathway in the injured dorsal root ganglion cell. Mol Med Rep 21:2385–2394
12. Conta G, Libanori A, Tat T, Chen G, Chen J (2021) Triboelectric nanogenerators for therapeutic electrical stimulation. Adv Mater 33:2007502
13. Yong H, Jung S, Heo D, Choi W, Chung J, Cho S, Hwang P, Song H, Koh WG, Lee W, Lee S, Hong J (2021) Body-mediated energy loss conversion for personalized cell vitalization. Nano Energy 87:106209
14. Hwang D, Lee H, Lee J, Lee M, Cho S, Kim T, Kim H (2021) Micro-current stimulation has potential effects of hair growth-promotion on human hair follicle-derived papilla cells and animal model. Int J Mol Sci 22:4361
15. Sohn KM, Jeong KH, Kim JE, Park YM, Kang H (2015) Hair growth-promotion effects of different alternating current parameter settings are mediated by the activation of Wnt/b-catenin and MAPK pathway. Exp Dermatol 24:958–963
16. Tian J, Shi R, Liu Z, Ouyang H, Yu M, Zhao C, Zou Y, Jiang D, Zhang J, Li Z (2019) Self-powered implantable electrical stimulator for osteoblasts' proliferation and differentiation. Nano Energy 59:705–714
17. Long Y, Wei H, Li J, Yao G, Yu B, Ni D, Gibson AL, Lan X, Jiang Y, Cai W, Wang X (2018) Effective Wound Healing enabled by Discrete Alternative Electric Fields from Wearable Nanogenerators. ACS Nano 12:12533–12540
18. Hunckler J, de Mel A (2017) A current affair: electrotherapy in wound healing. J Multidisciplinary Healthc 10:179–194
19. Sõti C, Nagy E, Giricz Z, Vígh L, Csermely P, Ferdinandy P (2005) Heat shock proteins as emerging therapeutic targets. Br J Pharmacol 146:769–780
20. Hsiao Y-C, Jheng P-R, Nguyen HT, Chen Y-H, Manga YB, Lu L-S, Rethi L, Chen C-H, Huang T-W, Lin J-D, Chang T-K, Ho Y-C, Chuang E-Y (2021) Photothermal-irradiated polyethyleneimine–polypyrrole nanopigment Film-Coated Polyethylene Fabrics for Infrared-Inspired with pathogenic evaluation. ACS Appl Mater Interfaces 13:2483–2495
21. Grossman MC, Dierickx C, Farinelli W, Flotte T, Anderson RR (1996) Damage to hair follicles by normal-mode ruby laser pulses. J Am Acad Dermatol 35:889–894

22. Bolouki N, Hsu Y-N, Hsiao Y-C, Jheng P-R, Hsieh J-H, Chen H-L, Mansel BW, Yeh Y-Y, Chen Y-H, Lu C-X, Lee J-W, Chuang E-Y (2021) Cold atmospheric plasma physically reinforced substances of platelets-laden photothermal-responsive methylcellulose complex restores burn wounds. Int J Biol Macromol 192:506–515
23. Chen Y-H, Chuang E-Y, Jheng P-R, Hao P-C, Hsieh J-H, Chen H-L, Mansel BW, Yeh Y-Y, Lu C-X, Lee J-W, Hsiao Y-C, Bolouki N (2021) Cold-atmospheric plasma augments functionalities of hybrid polymeric carriers regenerating chronic wounds: in vivo experiments. Mater Sci Eng C 131:112488
24. Chen T-H, Chen W-P, Wang M-JJ (2014) The effect of air permeability and water vapor permeability of cleanroom clothing on physiological responses and wear comfort. J Occup Environ Hyg 11:366–376
25. Schuster KC, Suchomel F, Männer J, Abu-Rous M, Firgo H (2006) Functional and Comfort Properties of Textiles from TENCEL® Fibres resulting from the Fibres' water-absorbing nanostructure: a review. Macromol Symp 244:149–165
26. Restan MS, Pedersen ME, Jensen H, Pedersen-Bjergaard S (2019) Electromembrane extraction of unconjugated fluorescein isothiocyanate from solutions of labeled proteins prior to flow induced dispersion analysis. Anal Chem 91:6702–6708
27. Satapathy MK, Nyambat B, Chiang C-W, Chen C-H, Wong P-C, Ho P-H, Jheng P-R, Burnouf T, Tseng C-L, Chuang E-Y (2018) A gelatin hydrogel-containing nano-organic PEI–Ppy with a photothermal responsive effect for tissue engineering applications. Molecules 23:1256
28. Bevilacqua M, Dominguez L, Barrella M, Barbagallo M (2007) Induction of vascular endothelial growth factor release by transcutaneous frequency modulated neural stimulation in diabetic polyneuropathy. J Endocrinol Investig 30:944–947
29. Bocchi L, Evangelisti A, Barrella M, Scatizzi L, Bevilacqua M (2010) Recovery of 0.1 hz microvascular skin blood flow in dysautonomic diabetic (type 2) neuropathy by using frequency rhythmic electrical modulation system (FREMS). Med Eng Phys 32:407–413
30. Cramp A, Gilsenan C, Lowe A, Walsh D (2000) The effect of high-and low-frequency transcutaneous electrical nerve stimulation upon cutaneous blood flow and skin temperature in healthy subjects. Clin Physiol (Oxford, England) 20:150–157
31. Atalay M, Oksala N, Lappalainen J, Laaksonen DE, Sen CK, Roy S (2009) Heat shock proteins in diabetes and wound healing. Curr Protein Pept Sci 10:85–95
32. Garnier C, Barbier P, Devred F, Rivas G, Peyrot V (2002) Hydrodynamic properties and quaternary structure of the 90 kDa heat-shock protein: effects of divalent cations. Biochemistry 41:11770–11778
33. Spierings J, van Eden W (2017) Heat shock proteins and their immunomodulatory role in inflammatory arthritis. Rheumatology 56:198–208
34. Venegas-Rodríguez R, Serrano-Díaz A, Peña-Ruiz R, Santana-Sánchez R, Hernández-Cedeño M, Rittoles Navarro A, Grecesqui-Cruz I, Pérez-Aguilera L, Segura-Fernández A, Rosario-Cruz L, Martínez-Donato G, Guillén-Nieto G, Domínguez MdC (2023) Horta, Jusvinza, an anti-inflammatory drug derived from the human heat-shock protein 60, for critically ill COVID-19 patients. An observational study. PLoS ONE 18:e0281111
35. Lopez T, Wendremaire M, Lagarde J, Duquet O, Alibert L, Paquette B, Garrido C, Lirussi F (2022) Wound Healing versus Metastasis: Role of Oxidative Stress. In: Biomedicines
36. Dunnill C, Patton T, Brennan J, Barrett J, Dryden M, Cooke J, Leaper D, Georgopoulos NT (2017) Reactive oxygen species (ROS) and wound healing: the functional role of ROS and emerging ROS-modulating technologies for augmentation of the healing process. Int Wound J 14:89–96
37. Kasuya A, Ito T, Tokura Y (2018) M2 macrophages promote wound-induced hair neogenesis. J Dermatol Sci 91:250–255

Publisher's Note Springer Nature remains neutral with regard to jurisdictional claims in published maps and institutional affiliations.

Springer Nature or its licensor (e.g. a society or other partner) holds exclusive rights to this article under a publishing agreement with the author(s) or other rightsholder(s); author self-archiving of the accepted manuscript version of this article is solely governed by the terms of such publishing agreement and applicable law.